Environ Fluid Mech (2013) 13:125–144
DOI 10.1007/s10652-012-9260-5

New analytical formulations for calculation of dispersion parameters of Gaussian model using parallel CFD

M. Ebrahimi · A. Jahangirian

Received: 29 March 2012 / Accepted: 4 November 2012 / Published online: 22 November 2012

Abstract New analytical formulations are presented for calculation of most effective parameters in the Gaussian plume dispersion model; the standard deviations of concentration for horizontal and vertical dispersion in neutral atmosphere conditions. Employing parallel Computational Fluid Dynamics (CFD) as a powerful tool, some well-known analytical generations of Pasquill–Gifford–Turner experimental data are modified. To achieve this aim, CFD simulations are carried out for single stack dispersion on flat terrain surface and ground level concentrations are determined in different distances. An inverse procedure in Gaussian plume dispersion model is then applied and standard deviations of horizontal and vertical dispersions are obtained. The values are compared with those of the well-known methods of Doury, Briggs and Hanna in two cases: the experimental data for release of krypton-85 from 100 m high and pollution dispersion from three 28 m high stacks of Besat power plant near Tehran. The comparison indicates that new formulations for plume dispersion are more accurate than other well-known formulations.

Keywords Air pollution · Gaussian model · Dispersion parameters · Parallel CFD · Analytical formulation

Abbreviations

CFD	Computational Fluid Dynamics
RANS	Reynolds Averaged Navier–Stokes
CALAUT	Computational Aerodynamic Laboratory at Amirkabir University of Technology
C	Convection
TD	Turbulent diffusion
MD	Molecular diffusion

M. Ebrahimi · A. Jahangirian (✉)
Department of Aerospace Engineering, Center of Excellence in Computational Aerospace, Amirkabir University of Technology, 424 Hafez Avenue, Tehran, Iran
e-mail: ajahan@aut.ac.ir

SP	Stress production
BP	Buoyancy production
PS	Pressure strain
DR	Dissipation rate
RC	Relative concentration
FB	fractional bias
MG	Mean geometric
NMSE	Normalized mean square error
VG	Geometric variance

1 Introduction

When an effluent plume is released to the atmosphere, it is transported downwind as a result of the mean wind field and simultaneously, diffused in a domain, due to the fluctuating wind components. Consequently the plume is spread in both the horizontal and vertical dimensions. The nature of such dispersion is of interest, especially for its wide range of consequences for human health. Thus, during the last decades much effort has been made to understand the nature of the pollution dispersion. The Gaussian plume dispersion model which is mathematically drived from advection–diffusion equations is one of the most important methods that is widely used to estimate pollution levels. This model have been applied extensively in the study of emissions from large industrial operations as well as a variety of other applications including release of radionuclide in atmosphere [30]; seed, pollen and insect dispersal [35]; and odor propagation from livestock facilities [42,50].

The most important parameters in this model which mainly impact the results are the standard deviation of vertical and horizontal dispersion of plume. The first considerable effort to estimate these parameters was carried out by Pasquill [38] who developed the stability categories from meteorological parameters. He presented a set of graphs to display these parameters as a function of downwind distance and stability class. Later, Gifford [20] utilized the same data as Pasquill, though changed the plume spreading parameters to the values of the concentration distribution. The result led to curves that we refer to as Pasquill and Gifford curves. These curves published in an EPA workbook by Turner [44], are based on the experimental data taken at distances of less than 1 km, then extrapolated out to greater distances. However with the advent of computers, it has become necessary to represent these observational curves with algebraic formula. Thus, much effort has been placed into best fit representations. Among them the most important ones are [9,16,23]. The more recent studies include [14,17,21,22,39,49]. However, their complications and dependence on parameters like turbulence data, heat and momentum fluxes and so on made them difficult to be implemented, in spite of their theoretical basis.

A distinct advantage of the Gaussian plume model is its simplicity as well as its speed; also this model allows the differentiation among the amount of pollutants which come from static or dynamic sources. In this model, parameter values are related to readily measurement quantities such as stack gas exit velocity and temperature, the temperature of the surrounding air and wind speed which made this model popular and relatively easy to apply. It is also considered suitable where the end points of the calculations are long term average or time integrated concentration in air, as is normally the case in the assessment of relative concentration from continuous releases. In addition to significant merits of this method, there are some demerits resulting in the appearance of new generations, such as the models do not

predict hourly observations at a specific time and the location beyond the immediate vicinity of the release, or model cannot track changing meteorological conditions.

The new generation models like UK-ADMS [12], ISC [47], Aeromode [48] and similar computerized packages are some instances which besides CFD modeling are used to simulate air pollution dispersion. One of the most significant works in this field is reported by AIJ group [1] in which they compared more than 60 sets of wind tunnel tests with numerical simulations results using a variety of numerical methods and turbulence models. They reported several important points and also showed that the skill in predicting flow varied widely. Latter Meroney et al. [37] extended their work by four additional sets of wind tunnel tests for air pollution dispersion and showed that Reynolds stress turbulent model (RSM) produces somewhat more realistic results than the Renormalization-Group (RNG) or k-ε models. However, the numerical simulations appear some disadvantages that causes Gaussian model to be still widely in use. First of all meteorological conditions are constantly changing like the speed and wind direction, sun radiation, ambient temperature, cloud density and so on that leads us not to have an absolute modeling. Secondly and the most important demerit is the requirement of much expertise, time to set up and large computing resources to run the model. Finally, changing geometry is inevitable that can completely deviate the estimation occurred by the model. On the contrary, Gaussian dispersion model can easily estimate the pollution concentration scale, especially with the precise value in a flat or slightly high terrain.

The main purpose of this paper is to increase the accuracy of Gaussian model by introducing new formulations for standard deviation of vertical and horizontal dispersion of plume for neutral atmospheric conditions. To achieve this, parallel Computational Fluid Dynamics simulations are carried out and the atmospheric boundary layer flows are simulated. The dispersion of a passive discharge from a single isolated stack for different input conditions is calculated which is a well understood case [5,40,41]. CFD results are then used as input data for Gaussian plume dispersion model. Then an inverse procedure is applied and standard deviations of horizontal and vertical dispersion are modified which results in new data. Then curves are fitted to these data so that new analytical formulations are concluded as well.

2 Methodology review

In the proposed procedure four major steps are carried out to increase the accuracy of Gaussian plume dispersion model. These steps are listed as below:

(1) Numerical modelings of dispersion of a passive discharge from a single isolated stack for different input conditions (i.e., inlet velocity profile, dimensions of stack and temperature of air and outlet plume).
(2) Determining relative concentration for at least 40 random points of the domain for each case.
(3) Calculation of vertical and horizontal dispersion coefficients using relative concentration values obtained from step 2 and Gaussian model (inverse procedure).
(4) Fitting curves to determine vertical and horizontal dispersion coefficients in order to obtain new formulations.

At the end the results are validated with the experimental data and well-known CFD cases. The following sections describe the above steps in detail.

2.1 Numerical modelings of dispersion from a single isolated stack

2.1.1 Governing flow equations and turbulence model

Governing equations of the flow field are the Reynolds' Averaged Navier–Stokes (RANS) equations. The conservation of the mass and momentum equations are given as following:

$$\frac{\partial}{\partial x_j} u_j = 0 \tag{1}$$

$$\frac{\partial}{\partial t} u_i + u_j \frac{\partial}{\partial x_j} u_i = -\frac{1}{\rho} \frac{\partial}{\partial x_i} P - \frac{\partial}{\partial x_j} \overline{u_i' u_j'} + \upsilon \frac{\partial^2}{\partial x_i \partial x_j} u_i \tag{2}$$

where $u_{i,j}$ are the mean fluid velocities in the x and y directions respectivly, P the mean pressure, ρ the fluid density, υ the kinematic viscosity and $u'_{i,j}$ are the fluctuation velocities. In Eq. (2) $\overline{u'_j u'_j}$ is the Reynolds stress tensor divided by fluid density. In this study, Reynolds stress model with a linear pressure–strain and wall-reflection effect has been applied [19, 26,27]. The wall-reflection term ensures redistribution of the normal stresses near the wall. It tends to damp the normal stress perpendicular to the wall while enhancing the stresses parallel to the wall. The energy equation is also given by the following:

$$\frac{\partial}{\partial t}(\rho E) + \frac{\partial}{\partial x_i}[u_i(\rho E + p)] = \frac{\partial}{\partial x_j}\left[\left(k + \frac{c_p \mu_t}{\mathrm{Pr}_t}\right)\frac{\partial T}{\partial x_j} + u_i(\tau_{ij})\right] \tag{3}$$

where E is the total energy, k the molecular conductivity, c_p the constant specific heats at constant pressure, μ_t the turbulent viscosity, Pr_t the Prandtl number, T the temperature and τ_{ij} is viscous stress tensor. For species transport the steady-state RANS equations supplemented with the Eulerian advection–diffusion equation are the governing equations which can be summarized in a tensor form as:

$$u_j \frac{\partial C}{\partial x_j} = \frac{\upsilon_t}{Sc_t} \cdot \frac{\partial^2 C}{\partial x_i \partial x_j} \tag{4}$$

where C is the mean mass fraction of the pollutant, u the mean velocity and υ_t/Sc_t is turbulent diffusion. The turbulent viscosity, υ_t, obtained from RSM turbulence model and turbulent Schmidt number Sc_t (the ratio of momentum diffusivity to mass diffusivity) should be determined prior to the numerical simulation. In the present research following the works of Li and Stathopoulos [33] and Wang and McNamara [51] the value of 0.7 is chosen for this number. Results show that, this value lead to more accurate standard deviations of horizontal and vertical dispersion. The second-order upwind model [2] is used for the pressure terms and the QUICK scheme [31] is used for all other ones.

2.1.2 Boundary conditions

For simulation of plume dispersion in atmosphere different types of boundary conditions are applied. The inlet plane and surface of stack outlet are specified as velocity inlet boundaries. Vertical and the top of the domain specify as symmetry (zero shear slip) and the outlet plane is specified as the pressure outlet plane.

For the ground surface, the standard wall function [28] with a roughness modification which is based on sand-grain is utilized. Such wall function in order to have the atmosphere boundary layer as input; need the equivalent sand-grain roughness height ($K_{S,ABL}$) which

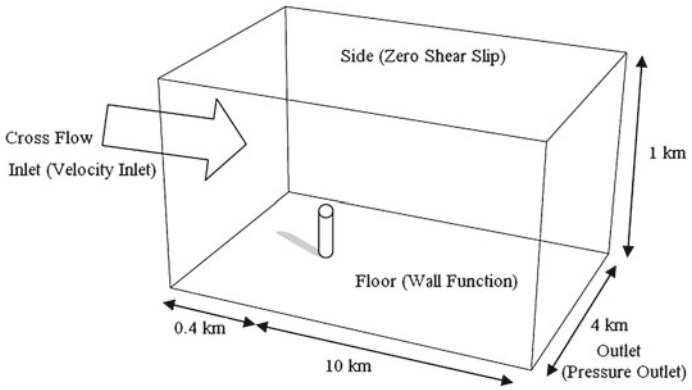

Fig. 1 Scheme of domain characteristics for all CFD cases

could be determined from roughness length (Z0) and roughness constant (CS). In this work the value of 0.1 and 0.5 are taken for roughness length and roughness constant, respectively [3]. The velocity profile in the inlet plane for a flat terrain is defined as following [11]:

$$u(z) = \frac{u^*}{\kappa} Ln\left(\frac{Z + Z_0}{Z_0}\right) \tag{5}$$

where u(z) is the wind speed, u* the friction velocity, κ the von Karman's constant taken to be 0.4 and Z_0 the surface roughness length.

2.1.3 Computational grid

The characteristic of the domain for all CFD cases are illustrated in Fig. 1. For minimizing the influences of the boundaries on the results of numerical modelings; the domain sizes is taken equal or larger than the one suggested by the Cost Action 732 guideline [18]. As indicated in Fig. 2, unstructured high resolution grids around the discharge of stacks is applied which is gradually converted to a structured low resolution grid far enough from the stack. The grids also have greater resolution close to the ground near the stack.

To obtain a suitable computational grid in term of resolution of points, the grid sensitivity study is carried out. Thus, three computational grids with different resolutions are generated named as coarse, medium and fine grids, with the 3448210, 5342218 and 7260311 grid cells.

A sample case with the input parameters of; U = 5(m/s), H = 100(m), D = 3(m), Vs = 3(m/s) and Q = 1(g/s) is defined. The Relative Concentration (RC) values obtain for the coarse and fine grids compared with those of the medium grid in Fig. 3. As illustrated the medium and fine grid results are consistent with each other while the coarse grid results are different. Thus, in this work for all CFD cases the M grid is utilized for modeling plume dispersion.

2.2 Calculation of relative concentration

According to the procedure described in Sect. 2.1, numerical modelings of dispersion from a single isolated stack for different input conditions (i.e., inlet velocity profile, dimensions of stack and temperature of air and outlet plume) are performed. For each case at least 40 random points within the domain are created and the relative concentrations in these points

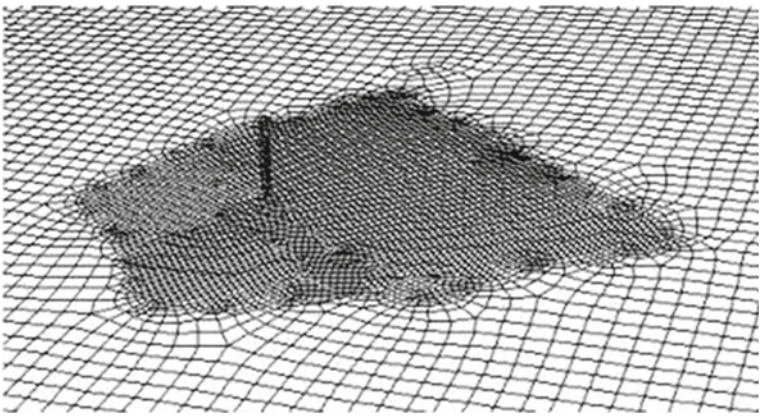

Fig. 2 The computational grid around the single stack and the ground surface vicinity

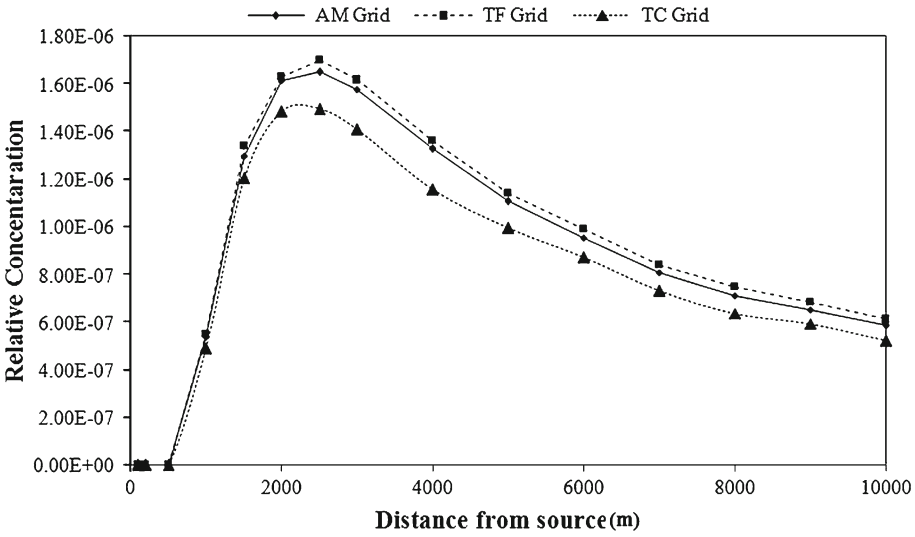

Fig. 3 Grid sensitivity analysis: concentration values obtained for a sample case [(U = 5(m/s), H = 100(m), D = 3(m), Vs = 3(m/s) and Q = 1(g/s)] with the Medium (*M*), coarse (*C*) and fine (*F*) grids

are opted from CFD simulations. Figure 4, shows the profile of the velocity in the different distances of inlet plane both in the lower 40 m and full height of boundary layer for friction velocity of 0.5 as an example of neutral atmospheric condition. This figure also shows that the near ground velocity gradient gradually increases with the distances; however the overall mean velocity profile approximately keeps its shape.

As mentioned earlier, in this paper the RSM turbulence model is applied for simulating turbulent characteristics. Figure 5a, b shows the Turbulent Kinetic Energy (TKE) and the dissipation rate profile at different distances from the inlet plane for a sample case (U = 5(m/s), H = 100(m), D = 3(m), Vs = 3(m/s) and Q = 1(g/s)—see Sects. 2.3 and 2.4 for the definitions of the parameters). These figures indicate that the TKE levels decreases with the distance near ground; in contrast such parameter increases along the domain with the increase in height

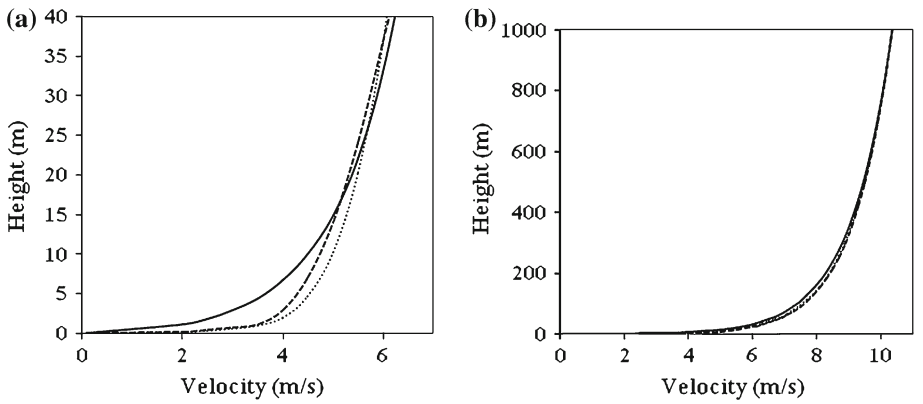

Fig. 4 The comparison between inlet velocity profile and its development of 3, 5 and 8 km downwind from inlet, **a** near ground, **b** full height of boundary layer for neutral atmosphere condition Dissipation (m^2 s^{-3})

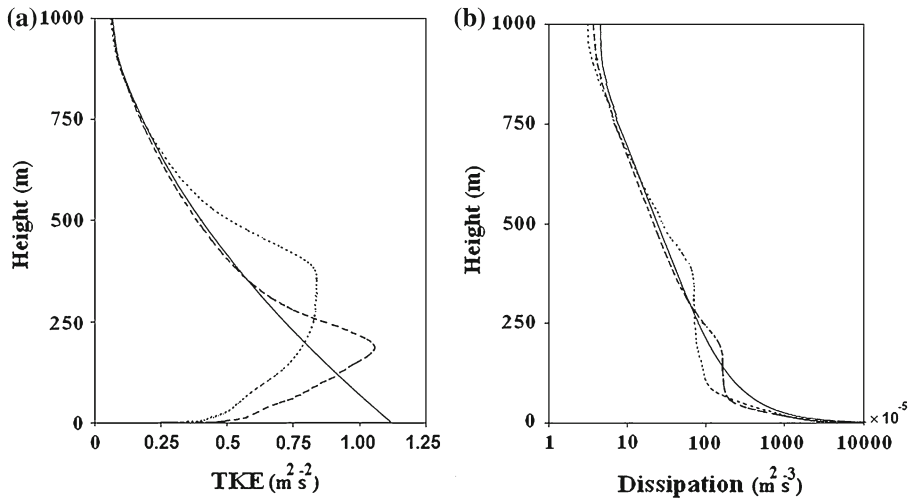

Fig. 5 The comparison between **a** inlet TKE and **b** dissipation rate profile and its development of 3 and 5 km downwind of inlet (**a**) near ground, (**b**) full height of boundary layer for neutral atmosphere condition.

while Dissipation approximately keeps its rate and shows only some fluctuations throughout the length of the domain.

2.3 Evaluation of dispersion coefficients

The Gaussian model is mathematically derived from advection–diffusion equations which for sources releasing continuously under steady-state conditions and ground reflection consideration is given as [45]:

$$C(x, y, z, H) = \frac{Qe^{\frac{-y^2}{2(\partial_y)^2}}}{2\pi\,\partial_y \partial_z U}\left[e^{\left(-\frac{(H-Z)^2}{2(\partial_z)^2}\right)} + e^{\left(-\frac{(H+Z)^2}{2(\partial_z)^2}\right)}\right] \tag{6}$$

Table 1 Dispersion parameters for neutral atmosphere conditions (Briggs model)

Surface cond.	Horizontal dispersion parameter σ_y(m)			Vertical dispersion parameter σ_z(m)		
	a	b	c	a	b	c
Open country cond.	0.08	0.0001	−0.5	0.06	0.0015	−0.5
Urban country cond.	0.16	0.0004	−0.5	0.14	0.0003	−0.5

where C is the air pollutant concentration (g/m^3), Q the source emission rate (g/s), U the wind speed at the height of effective plume rise (m/s), x the distance from the source in meter, H the effective plume rise (m) and ∂_y, $\partial_z$are lateral and vertical dispersion coefficients. According to [45], this model should be able to predict concentration distributions within a factor of 3. The effective plume rise is calculated based on [25] formulation which defined as physical height of stack (H_s) plus the plume rise (H_p):

$$H_p = \frac{V_s d}{U}\left(1.5 + 2.68 \times 10^{-3} p_0 \frac{\Delta T}{T_s} d\right) \tag{7}$$

where V_s is the stacks outlet gas speed (m/s), d the inner stack diameter plume (m), p_0 ambient pressure value (mbar), and T_s outlet gas temperature (°k) and ΔT the difference of T_s with ambient temperature. For momentum ratios $M_r = Vs/U > 1.5$ the maximum plume rise is $3d \times M_r$ [8]. Note that the wind speed, U, is at height H.

2.3.1 Briggs model

Briggs [7] proposed a series of algebraic interpolation formulas for both rural and urban terrain based on various types of data [10,43] which have become widely known. The formulation and its coefficients for neutral atmospheric conditions are given in Eq. 8 and Table 1, respectively.

$$\partial_y \; or \; \partial_z = ax(1 + bx)^c \tag{8}$$

2.3.2 Doury model

Out of a review of experimental data [6,15,16,29] derived a relationship between dispersion coefficients and the travel time, t, as:

$$\partial_y \; or \; \partial_z = A(t)^k \tag{9}$$

In this formula two variations of dispersion coefficients are considered and categorized as normal and weak diffusion. The value of A and k coefficients for a variety of time travel in normal atmospheric conditions considered in this research is given in Table 2.

2.3.3 Hanna et al. model

Hanna and Drivas [23] suggested an analytical formulation on Pasquill–Gifford experimental data, which is mentioned in the following,

$$\partial_y \; or \; \partial_z = ax^b + c \tag{10}$$

Table 2 Dispersion parameter for neutral atmosphere conditions (Doury model)

Transfer time (s)	A_x or A_y (m)	A_z (m)	K_x or K_y (m)	K_z (m)
0–240	0.405	0.42	0.859	0.814
240–3280	0.135	1	1.130	0.685
3280–97E03	0.135	20	1.130	0.500
97 E03–508 E03	0.463	20	1.000	0.500
508 E03–13E05	6.500	20	0.824	0.500
>13E05	2E05	20	0.500	0.500

Table 3 Dispersion parameter of The Hanna model for neutral atmosphere conditions

Horizontal dispersion parameter σy (m)			Vertical dispersion parameter σz (m)		
a	b	c	a	b	c
0.068	0.908	0	0.066	0.915	0

Table 4 Domain of validation of proposed formulations based on atmospheric stability classes for use with the Pasquill–Gifford dispersion model

Wind speed (m/s)	Day radiation intensity			Night cloud cover	
	Strong	Medium	Slight	Cloudy	Clear
<2	A	A–B	B	F	F
2–3	A-B	B	C	E	F
3–5	B	B–C	C	D	E
5–6	C	C–D	D	D	D
>6	C	D	D	D	D

A very unstable, *B* moderately unstable, *C* slightly unstable, *D* neutral, *E* moderately stable, *F* very stable

The coefficients a, b and c for neutral atmospheric conditions are given in Table 3. Although better algebraic fits are possible, this model is still widely in use.

2.4 The proposed model

In this work, the aim is to derive new mathematical formulations for standard deviation of horizontal and vertical dispersion in neutral atmospheric conditions. Table 4 highlights the domain of validation of the proposed formulations based on Pasqual-Gifford stability class. The velocity is measured in 10 m height so in the majority of cases the present formulations are valid.

To derive new formulations (Fitting curves) for standard deviation of dispersion which accurately predicts pollution concentration in Gaussian plume model in comparison to other well-known models, an inverse procedure is applied.

In the numerical modeling part of this research, several cases are built in which for each case input conditions including inlet boundary layer velocity profile ($0.5 < u^* < 1.5$), ambient temperature ($5 < Ta < 27$), height ($20 < H < 100$) and diameter ($0.5 < D < 3$) of the stack, outlet velocity ($4 < Vs < 12$) and the temperature ($80 < Ts\ (c) < 140$) of released gas are

Table 5 Dispersion parameter of The present model for neutral atmosphere conditions

Horizontal dispersion parameter σy (m)				Vertical dispersion parameter σz (m)					
a	b	c	d	a	b	c	d	e	f
−2.459E−06	2	7.080E−02	1.278	1.623E−10	3	−4.164E−06	2	4.150E−02	38.310

varied. Then concentrations for random distances from the stack in stream-wise, span-wise and vertical directions are determined. In each case, at least 40 points are chosen from those 10 points are selected for 100–300 m and 10 points for last 100 m of the domain, others are randomly chosen from other parts of the domain. Since the plume rise from a stack occurs over some distance downwind, Gaussian plume model should not be applied within the first hundred meters from the stack.

Then an inverse procedure is applied so that air pollutant concentration is the input and unknowns are only dispersion coefficients. Since there will be two unknown parameters of σ_y and σ_z in each equation for each point, there is not a unique solution for that. To obtain an approximation of these coefficients, least square method is applied, with initial value of Briggs model. MacKay et al. [36] used a similar least square method to estimate parameters such as surface mass transfer rate and Peclet number rather than emission rates. Then the new curves are fitted as:

$$\partial_y = ax^b + cx + d \tag{11}$$

$$\partial_z = ax^b + cx^d + ex + f \tag{12}$$

The coefficients of proposed formulations are given in Table 5.

These curves are shown in Fig. 6 in comparison with the Briggs, Doury and Hanna results. As noted before in Gaussian model, the above equations should not be applied in the first 100 m from the stack because the plume rise occurs over some distance downwind. Table 6 shows the description of the method to calculate standard deviations of horizontal and vertical dispersions for three random points.

3 Results

To assess the applicability and accuracy of the presented formulations, two cases are applied. The first case is an experimental study of releasing krypton-85 from 100-m-high stack above a complex coastal terrain at La Hague reported by Leroy et al. [32]. The second case is numerical pollutant dispersion from three 28-m-high stacks of Besat power plant near Tehran. To be able to evaluate the results independent of the volume of the pollutant flow from source(s), the parameter of Relative Concentration is applied as following:

$$RC = \frac{C(g/m^3)}{Q(g/s)} \tag{13}$$

where C and Q are the same as defined in Eq. 6. In order to compare the accuracy of the method, a statistical method of Hanna et al. [24] is applied. The following equations define the statistical performance measures, which include the fractional bias (FB), the geometric mean bias (MG), the normalized mean square error (NMSE), the geometric variance (VG) and the fraction of predictions within a factor of two of observations (FAC2):

Table 6 The description of the method to calculate standard deviations of horizontal and vertical dispersions for three random points

Locations of calculation			Wind vel.	Release height	Diam.	T_a	T_o	U_o	C/Q	σ_y	σ_z
x (km) Variable from 0 to 10	y (km) Variable from 0 to 4	z (km) Variable from 0 to 1	U (m/s) <5	H (m) Determine effective plume rise	D(m)	(°C)	(°C)	(m/s)	$(S\,m)^{-3}$ Calculated from CFD	(m) Guessed to satisfy numerical value based on Gauss model	(m)
500.0	0.0	0.3	7	30	3	27	120	10	6.0E−06	47.1	24.3
1000.0	100.0	0.3	7	50	2	27	110	12	2.3E−06	80.9	40.2
2000.0	0.0	100.0	7	100	2	27	100	15	2.3E−06	142.5	68.7

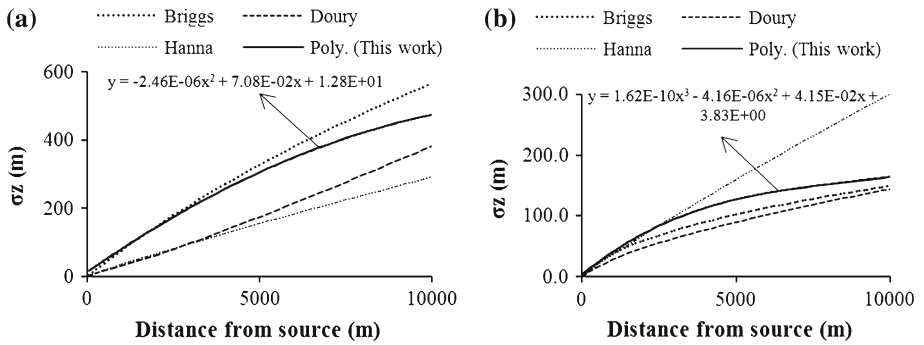

Fig. 6 Dispersion coefficients for neutral atmospheric condition based on Pasqual–Gifford stability class **a** horizontal dispersion and **b** vertical dispersion

$$FB = \frac{(\overline{C_0} - \overline{C_p})}{0.5(\overline{C_0} + \overline{C_p})} \tag{14}$$

$$MG = \exp(LnC_o - LnC_p) \tag{15}$$

$$NMSE = \frac{\overline{(C_o - C_p)}^2}{\overline{C_o C_p}} \tag{16}$$

$$VG = \exp[(\overline{LnC_o - LnC_p})^2] \tag{17}$$

$$FAC2: \frac{1}{2} \leq \frac{C_p}{C_o} \leq 2 \tag{18}$$

where $\overline{C}$ is the average over the data set, Cp is Gaussian model predictions and C_o is concentration measured by CFD. A perfect model has MG, VG, and FAC2 equal to 1.0; and FB and NMSE equal to 0.0 [13]. The FB indicates how well the computation produces the average values around the average values of observed variable. The ideal value of this measure is zero, but it can range from 2 to −2, The NMSE gives information on the strengths of deviations and not on the over or under prediction thus, always giving positive values. Differences on peak values have a higher weight on NMSE than differences on other values. For example, the linear measures FB and NMSE can be overly influenced by infrequently occurring high observed or predicted concentrations, whereas the logarithmic measures MG and VG may provide a more balanced treatment of extreme high values.

3.1 Release of krypton-85 from nuclear plant at La Hague

The French Institute for Radiological Protection and Nuclear Safety (IRSN) in 2001–2002 studied the behavior of atmospheric dispersion of 15 releases from the nuclear fuel reprocessing plant AREVA NC-La Hague, using the chemically inert gas krypton-85, as a tracer for plumes emitted from 100-m-high stack. Concentration measurements were carried out at neutral or slightly unstable atmospheric conditions and σ_y were determined from these measurements. Table 7 shows the measured and calculated values of dispersion coefficients by the proposed and different other formulations [32]. The values of 13 campaigns which were measured in neutral conditions in comparison to calculated values of this work formulation shows a great capability of predicting $\sigma_y$in different distances.

Table 7 The standard deviation of dispersion for different conditions

Camp.	Wind speed (m/s)	Stab. class	Dist. (m)	σ_y					σ_z			
				Exp. [32]	This work	Briggs	Doury	Hanna	This work	Briggs	Doury	Hanna
D9_2	9.7	D	360	40	37.9	28.3	10.0	14.2	18.2	17.4	9.1	14.4
D9_1	10.7	D	550	54	51.0	42.8	13.6	20.9	25.4	24.4	12.2	21.2
D10_1	9.3	D	575	60	52.7	44.7	15.9	21.8	26.3	25.3	14.2	22.1
D2_1	11.7	D	600	43	54.4	46.6	13.5	22.7	27.3	26.1	12.2	23.0
D4_1	9.0	D	620	60	55.7	48.1	17.4	23.3	28.0	26.8	15.5	23.7
D7_1	13.6	D	625	52	56.1	48.5	12.3	23.5	28.2	26.9	11.1	23.9
D1_1	12.2	D	950	80	77.8	72.6	19.4	34.4	39.6	36.6	17.1	35.0
D1_2	11.8	D	1,000	82	81.1	76.3	20.8	36.0	41.3	37.9	18.3	36.7
D8_1	14.4	D	1,100	105	87.7	83.5	19.1	39.3	44.7	40.5	16.8	40.0
D3_1	5.1	C	1,200	105	94.2	90.7	50.1	42.5	47.9	43.0	2.1	43.4
D6_1	13.6	D	1,850	160	135.3	136.0	31.3	63.0	67.4	57.1	26.9	64.4
D4_2	6.8	D	2,300	143	162.6	165.9	75.0	76.7	79.2	65.4	54.0	78.6
D10_2	8.2	D	2,600	190	180.2	185.3	69.8	85.8	86.4	70.5	51.7	88.0
D5_1	7.1	C	3,100	210	208.6	216.7	100.1	100.6	97.3	78.3	64.3	103.3
D11_1	16.3	D	3,260	200	217.5	226.5	43.6	105.3	100.5	80.6	36.8	108.2

Table 8 Statistical evaluations of the present work, Briggs, Doury, Hanna models and experimental data of nuclear fuel reprocessing plant La Hague

Parameter	FB	MG	NMSE	VG	FAC2
This work	0.020	1.023	0.012	1.013	1.000
Briggs	0.046	1.106	0.021	1.032	1.000
Doury	0.801	2.480	0.945	2.337	0.133
Hanna	0.762	2.324	0.851	2.074	0.200

Table 9 The physical features of the stacks of the Besat power plant with its pollution emission

Stack no.	Height (m)	Diam. (m)	Outlet gas vel. (m/s)	T (°C)	Volumic flow (m^3/s)
First	30	2.85	12.5	375	79.7
Second	30	2.85	12.8	382	81.7
Third	30	2.85	12.2	371	77.8

The performance statistics for these data are shown in Table 8. This table shows that the new formulation on lateral standard deviation of dispersion outperforms the other well-known models of Briggs, Doury and Hanna. Positive FB in this table also indicates that all models under predict σ_y specifically Doury and Hanna. However, the new formulation gives the best agreement with the observed mean and standard deviation. The new formulation also shows a better performance in the MG, NMSE, VG and FAC2 statistics. It should be noted that if FAC3 is used instead of FAC2, these values are 1 for all models which means that all data are approximately within the range.

3.2 Pollutant dispersion from Besat power plant

The second test is the calculation of the pollution dispersion from three 28-m height stack of Besat gas power plant located in the south of Tehran. The area is known as one of the most polluted parts of the Tehran. Due to the existence of several pollutant sources including rail station, gas refinery plant and also this old power plant, it is impossible to distinguish the portion of emission of pollutant gases from Besat's Stacks with other sources. Then instead of using the measurement device, CFD simulation for modeling plum dispersion is applied which its specifications are described in the following.

The physical features of the stacks of the Besat power plant with its pollution emission are presented in Table 9. The site plant is 560 m long and 350 m wide in north-south and west-east directions, respectively.

For the CFD simulations of gas dispersion from the stacks of Besat power plant, a domain size and model like single stack described in Sect. 2.1 are applied. Because almost all buildings in this area are short and dense tangle, a surface roughness of 3 m is applied for outside the site whereas buildings inside the site are exactly modeled. The domain is discretized using an unstructured hexahedral grid in the vicinity of stacks and buildings which is gradually converted into a structured low resolution grid in a distance from stacks. Figure 7, shows surface grid applied for the model. A high resolution grid is applied near the discharge positions because the pollutant concentrations are dependent upon the accuracy of the real plume spread rates.

Table 10 The value of RC up to 10 km from central stack of Besat power plant, wind speed at 10-m-height, ambient and outlet gas temperatures case (a) 7 (m/s), 300 (°k) and 410 (°k); case (b) 5.5 (m/s), 283 (°k) and 383 (°k)

Dist. from release (m)	Relative concentration									
	Numerical		This work		Briggs		Doury		Hanna	
	Case a	Case b	Case a	Case b	Case a	Case b	Case a	Case b	Case a	Case b
100	3.8E−08	1.6E−09	2.6E−11	9.6E−13	2.3E−18	2.3E−21	1.9E−28	8.8E−24	1.2E−26	2.1E−31
200	6.2E−07	2.4E−07	2.1E−07	5.5E−08	4.3E−08	7.2E−09	1.1E−11	3.3E−10	3.9E−10	2.1E−11
500	1.9E−05	1.5E−05	1.7E−05	1.4E−05	1.8E−05	1.5E−05	6.4E−06	1.2E−05	2.0E−05	1.4E−05
1000	2.1E−05	2.0E−05	2.1E−05	2.4E−05	2.2E−05	2.4E−05	3.7E−05	4.1E−05	4.6E−05	4.9E−05
1500	1.2E−05	1.7E−05	1.5E−05	1.8E−05	1.6E−05	1.8E−05	3.7E−05	3.5E−05	3.4E−05	3.9E−05
2000	1.0E−05	1.3E−05	1.1E−05	1.3E−05	1.1E−05	1.4E−05	2.9E−05	2.5E−05	2.3E−05	2.8E−05
2500	6.4E−06	9.5E−06	8.0E−06	9.8E−06	8.8E−06	1.1E−05	2.2E−05	1.9E−05	1.7E−05	2.1E−05
3000	5.6E−06	6.8E−06	6.3E−06	7.8E−06	7.0E−06	8.6E−06	1.7E−05	1.4E−05	1.3E−05	1.6E−05
4000	3.1E−06	4.5E−06	4.3E−06	5.4E−06	4.9E−06	6.0E−06	1.1E−05	9.1E−06	7.7E−06	9.7E−06
5000	2.8E−06	3.9E−06	3.3E−06	4.1E−06	3.7E−06	4.6E−06	7.6E−06	6.3E−06	5.3E−06	6.6E−06
6000	2.7E−06	3.0E−06	2.7E−06	3.4E−06	2.9E−06	3.6E−06	5.6E−06	4.7E−06	3.8E−06	4.8E−06
7000	1.9E−06	2.5E−06	2.3E−06	2.9E−06	2.4E−06	3.0E−06	4.3E−06	3.6E−06	2.9E−06	3.7E−06
8000	1.8E−06	2.5E−06	2.0E−06	2.6E−06	2.0E−06	2.5E−06	3.4E−06	2.9E−06	2.3E−06	2.9E−06
9000	1.6E−06	2.3E−06	1.8E−06	2.3E−06	1.7E−06	2.2E−06	2.8E−06	2.3E−06	1.9E−06	2.4E−06
10000	1.6E−06	2.1E−06	1.7E−06	2.1E−06	1.5E−06	1.9E−06	2.3E−06	1.9E−06	1.5E−06	1.9E−06

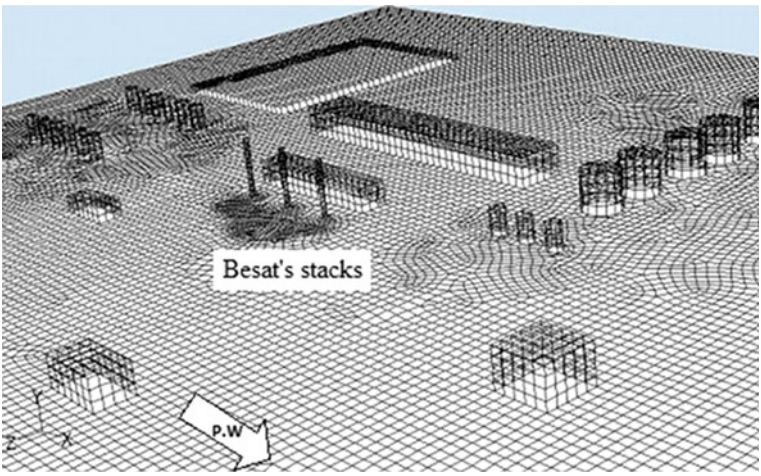

Fig. 7 Surface grid around the stacks of Besat power plant and prevailing west-east wind direction

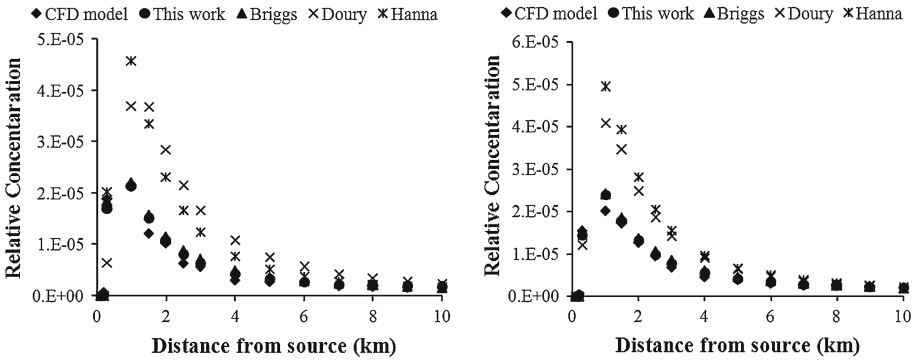

Fig. 8 The calculated values of RC for Gaussian model (Briggs, Doury, Hanna, present work) in comparison to CFD. wind speed at 10-m-height, ambient and outlet gas temperatures **a** 7 (m/s), 300 (°k) and 410 (°k); **b** 5.5 (m/s), 283 (°k) and 383 (°k)

Two flow conditions are applied for this case which, are within the range of the most possible neutral conditions in the area of based on the nearby meteorological station report. In the first case, the mean wind speed at 10-m-height is 7(m/s) and ambient and outlet gas temperatures are 300 (°k) and 410 (°k) respectively. In the second case the mean wind speed at 10-m-height is 5.5 (m/s) and ambient and outlet gas temperatures are 283 (°k) and 383 (°k). Table 10 shows the values of RC up to 10 km from central stacks of Besat power plant calculated by Briggs, Doury, Hanna and the proposed model in comparison to CFD results. The calculated and observed values of RC for two mentioned cases are plotted in Fig. 8, as a function of the distance to the central stack. This figure shows that, maximum concentration in neutral atmospheric conditions occur between 500 and 1,500 m of stacks in the prevailing wind directions.

Statistical evaluations on these data shown in Table 11 indicating that the formulations proposed in this work in all 5 factors achieve the best results where the worst predictions are for Doury and Hanna. Also the positive values of FB indicate that the RC is overestimated by all models. The number of calculated RC values which are within a factor of two for this

Table 11 Statistical evaluations of this work formulation, Briggs, Doury and Hanna models for RC at each point, wind speed at 10-m-height, ambient and outlet gas temperatures case a: 7 (m/s), 300 (°k) and 410 (°k); case b) 5.5 (m/s), 283 (°k) and 383 (°k)

Parameter	FB		MG		NMSE		VG		FAC2	
	Case a	Case b	Case a	Case b	Case a	Case b	Case a	Case b	Case a	Case b
This work	−0.07	−0.07	1.58	1.70	0.03	0.02	37.84	46.34	0.87	0.87
Briggs	−0.13	−0.11	4.96	7.07	0.05	0.03	Huge	Huge	0.87	0.87
Doury	−0.68	−0.53	25.00	9.69	1.63	0.88	Huge	Huge	0.27	0.60
Hanna	−0.65	−0.64	17.30	35.03	1.32	1.35	Huge	Huge	0.47	0.47

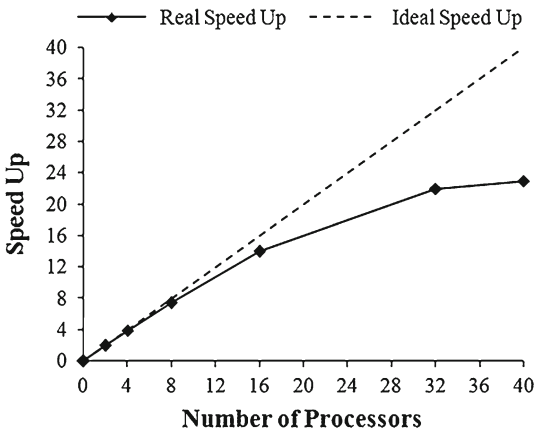

Fig. 9 Real and ideal speedup versus number of processors

work and Briggs are 13 of 15 (87 %) but checking the results reflects that the outputs of the present work are much closer to CFD values. The high values of the parameter VG for the Briggs, Doury and Hanna models in both cases indicate the low values of RC evaluated in near field for these models.

3.3 Parallelization

Since the domain size for modeling plume dispersion by CFD is very large and the problem is computationally intensive; parallelization is utilized. The grid is subdivided into several sub domains which are a function of the number of the processors with one-cell overlaps at the interfaces and RANS equations are solved for the sub domains. As illustrated in Fig. 9, the real speedup (defined as the computational time on 1 processor divided by the computational time on "N" processors) in comparison to ideal speedup decreases as the number of processors increases. In this work 32 processors are used.

The parallel computer system of Computational Aerodynamics Laboratory at Amirkabir University of Technology (CALAUT) is used which has 40 CPUs comprising five nodes, each node packing four processors on one motherboard. The system configuration is summarized in Table 12.

Table 12 Configuration of parallel computer of CALAUT

Unit	Configuration
CPU	AMD Opteron (Quad Core) 2.54 GHz
No. of CPUs	40 (5 nodes)
Hard disk	1 Terabytes
Memory	160 Gbytes
Network	Myrinet
Operating system	Linux (64-bit version)

4 Conclusions

In order to improve the accuracy of Gaussian plume model, new analytical formulations for standard deviation of horizontal and vertical dispersion were suggested. To achieve this aim, Computational Fluid Dynamics simulations were set up for a single stack. Then ground level concentrations were determined at different distances. Inverse procedure was applied and standard deviations of horizontal and vertical dispersion were modified which resulted in new formulations. Using a statistical method the results of the presented approach are show its superiority to the models of Briggs, Doury and Hanna.

References

1. Architectural Institute of Japan (1998) Working group for numerical predication of wind loading on buildings and structures. Subcommittee for wind engineering data unit for structural design. Numerical prediction of wind loading on buildings and structures
2. Barth TJ, Jespersen DC (1989) The design and application of upwind schemes on unstructured meshes. AIAA Paper No. 89–0366, 27th AIAA aerospace sciences meeting and exhibit, Reno, NV, USA.
3. Blocken B, Stathopoulos T, Carmeliet J (2007a) CFD simulation of the atmospheric boundary layer-wall function problems. Atmos Environ 41(2):238–252
4. Blocken B, Carmeliet J, Stathopoulos T (2007b) CFD evaluation of the wind speed conditions in passages between buildings—effect of wall-function roughness modifications on the atmospheric boundary layer flow. J Wind Eng Ind Aerodyn 95(9–11):941–962
5. Blocken B, Stathopoulos T, Saathoff P, Wang X (2008) Numerical evaluation of pollutant dispersion in the built environment: comparison between models and experiments. J Wind Eng Ind Aerodyn 96 (10–11):1817–1831
6. Bovard P, Caput, C, Doury A (1968) Etude expérimentale en vraie grandeur des transferts atmosphériques en terrain hétérogène accidenté. In: Congrès international sur la radioprotection du milieu devant le développement des utilisations pacifiques de l'énergie nucléaire, SFRP, Toulouse, Mai, pp 61–77
7. Briggs GA (1973) Diffusion estimation of small emissions. Contribution No. 79. Atmopsheric Turbulence and Diffusion Laboratory, Oak Ridge, TN
8. Briggs GA (1984) Plume rise and buoyancy effects. In: Anders R (ed) Atmospheric science and power production. U.S. Department of Energy D.O.E./TIC-27601 (DE 84005177), Washington, DC
9. Briggs GA (1985) Analytical parameterizations of diffusion—the convective boundary layer. J Clim Appl Met 14:1167–1186
10. Carpenter S, Montgomery TL, Leavitt JM, Colbaugh WC, Thomas FW (1971) Principal plume dispersion models: TVA power plants. J Air Pollut Control Assoc 21:491–495
11. Carruthers DJ (1994) UK-ADMS: a new approach to modeling dispersion in the Earth's atmospheric boundary layer. J Wind Eng Ind Aerodyn 52:139–153
12. Carruthers DJ et al (1992) UK Atmospheric Dispersion Modelling System (UK-ADMS). In: van Dop H, Kallos G (eds) Air pollution modeling and its application IX. Appendix A: boundary layer structure. Plenum Press, New York, pp 15–28
13. Chang JC, Hanna SR (2004) Air quality model performance evaluation. Meteorol Atmos Phys 87:167–196

14. Coirier WJ (2005) Evaluation of CFD codes—US perspective. In: Schatzmann M, Britter R (eds) Quality assurance of microscale meteorological models. COST 732 report. European Science Foundation, ISBN 3-00-018312-4
15. Doury A (1960) Météorologie et contrôle des radiations en atmosphère libre au voisinage d'un site nucléaire. La météorologie_IV_60_451-471
16. Doury A (1981) Le vadémécum des transferts atmosphériques. rapport n_CEA-DSN- 440. CEA
17. Erbrink JJ (1995) Turbulent diffusion from tall stacks. The use of advanced boundary-layer meteorological parameters in the gaussian dispersion model "STACKS". Ph.D. Thesis, Free University, Amsterdam, April 1995
18. Franke J, Hellsten A, Schlunzen H, Carissimo B (2007) Best practice guideline for the CFD simulation of flows in the urban environment. COST Action 732: quality assurance and improvement of microscale meteorological models
19. Gibson MM, Launder BE (1978) Ground effects on pressure fluctuations in the atmospheric boundary layer. J Fluid Mech 86:491–511
20. Gifford FA (1961) Use of routine meteorological observations for estimating atmospheric dispersion. Nucl Saf 2:47–57
21. Hanna S, Baja E (2009) A simple urban dispersion model tested with tracer data from Oklahoma City and Manhattan. Atmos Environ 43(2009):778–786
22. Hanna SR, Chang J (1993) Hybrid plume dispersion model (HPDM) improvements and testing at three field sites. Atmos Environ 27A:1491–1508
23. Hanna SR, Drivas PJ (1987) Guidelines for use of vapor cloud dispersion models. Center for chemical process safety. American Institute of Chemical Engineers, New York
24. Hanna SR, Strimaitis DG, Chang JC (1991) Hazard response modeling uncertainty (a quantitative method) volume I: user's guide for software for evaluating hazardous gas dispersion models. Sigma Research Corporation, Westford
25. Holland JZ (1953) A Meteorological Survey of the Oak Ridge Area. U.S. Atomic Energy Commission Report No. ORO-99. U.S. Government Printing Office, Washington DC
26. Launder BE (1989) Second-moment closure and its use in modeling turbulent industrial flows. Int J Numer Methods Fluids 9:963–985
27. Launder BE (1989) Second-moment closure: present.. and future? Int J Heat Fluid Flow 10(4):282–300
28. Launder BE, Spalding DB (1974) The numerical computation of turbulent flows. Comput Methods Appl Mech Eng 3:269–289
29. Le Quinio R (1964) Abaques pour le calcul de la pollution atmosphérique due aux effluents d'une source ponctuelle. Service de contrôle des radiations et de genie radioactif. Note CEA N_488
30. Leelossy A, Robert Meszaros R, Istvan Lagzi I (2011) Short and long term dispersion patterns of radionuclides in the atmosphere around the Fukushima Nuclear Power Plant. J Environ Radioact 102:1117–1121
31. Leonard BP, Mokhtari S (1990) ULTRA-SHARP nonoscillatory convection schemes for high-speed steady multidimensional flow. NASA TM 1-2568 (ICOMP-90-12), NASA Lewis Research Center
32. Leroy C, Maro D, Hébert D, Solier L, Rozet M, Le Cavelier S, Connan O (2010) A study of the atmospheric dispersion of a high release of krypton-85 above a complex coastal terrain, comparison with the predictions of Gaussian models. J Environ Radioact 101:937–944
33. Li Y, Stathopoulos T (1997) Numerical evaluation of wind-induced dispersion of pollutants around a building. J Wind Eng Ind Aerodyn 67&68:757–766
34. Li Y, Stathopoulos T (1998) Computational evaluation of pollutant dispersion around buildings: estimation of numerical errors. J Wind Eng Ind Aerodyn 77&78:619–630
35. Loos CC, Seppelt R, Meier-Bethke S, Schiemann J, Richter O (2003) Spatially explicit modelling of transgenic maize pollen dispersal and cross-pollination. J Theor Biol 22:241–255
36. MacKay C, McKee S, Mulholland AJ (2006) Diffusion and convection of gaseous and fine particulate from a chimney. IMA J Appl Math 71:670–691
37. Meroney RN, Leitl BM, Rafailidis S, Schatzmann M (1999) Wind-tunnel and numerical modeling of flow and dispersion about several building shapes. J Wind Eng Ind Aerodyn 81:333–345
38. Pasquill F (1961) Estimation of the dispersion of windborne material. Meteorol Mag 90:33–49
39. Pelliccioni A, Tirabassi T (2006) Air dispersion model and neural network: a new perspective for integrated models in the simulation of complex situations. Environ Model Softw 21:539–546
40. Raza SS, Avila R, Cervantes J (2001) A 3-D Lagrangian stochastic model for the meso-scale atmospheric dispersion applications. Nucl Eng Des 208:15–28
41. Riddle A, Carruthers D, Sharpe A, McHugh C, Stocker J (2004) Comparison between FLUENT and ADMS for atmospheric dispersion modeling. Atmos Environ 38:1029–1038
42. Schauberger G, Piringer M, Knauder W, Petz E (2011) Odour emissions from a waste treatment plant using an inverse dispersion technique. Atmos Environ 45:1639–1647

43. Singer IA, Smith ME (1966) Atmospheric dispersion at Brookhaven National laboratory. Int J Air Water Pollut 10:125–135
44. Turner DB (1967) Workbook of atmospheric dispersion estimates. Public Health Series. Publication 999-AP-26. Cincinnati, OH
45. Turner DB (1970) Workbook of atmospheric dispersion estimates. U.S. Environmental Protection Agency, Environment Health Series Air Pollution, 84, Research Triangle Park
46. Turner R, Hurst T (2001) Factors influencing volcanic ash dispersal from the 1995 and 1996 eruptions of Mount Ruapehu, New Zealand. J Appl Meteorol 40:56–69
47. USEPA (1995) Users guide to the Industrial Source Complex (ISC3) dispersion models (revised). Volume 1—user instructions. EPA-454/b-95-003a. US Environmental Protection Agency, Research Triangle Park, NC
48. USEPA (2003) AERMOD: latest features and evaluation results. EPA-454/R-03-003. US Environmental Protection Agency, Research Triangle Park, NC
49. Verwoerd WS (2011) New stochastic model for dispersion in heterogeneous porous media: 2. Gaussian plume transmission across stepwise velocity fluctuations. Appl Math Model 35:3355–3386
50. Vieira de Melo AM, Meri Santos J, Reis Junior NC (2012) Modelling of odour dispersion around a pig farm building complex using AERMOD and CALPUFF. Comparison with wind tunnel results. J. Build Environ 56:8–20
51. Wang X, McNamara KF (2006) Evaluation of CFD simulation using RANS turbulence models for building effects on pollutant dispersion. Environ Fluid Mech 6:181–202